Molecular Pharmacology Fast Forward. Published on June 13, 2005 as doi:10.1124/mol.105.014431
This article has not been copyedited and formatted. The final version may differ from this version.

MOL 14431

Effects of Quinine, Quinidine and Chloroquine on α9α10 Nicotinic Cholinergic Receptors

Jimena A. Ballestero, Paola V. Plazas, Sebastian Kracun, María E. Gómez-Casati, Julián Taranda, Carla V. Rothlin, Eleonora Katz, Neil S. Millar, and A. Belén Elgoyhen

Instituto de Investigaciones en Ingeniería Genética y Biología Molecular, Consejo Nacional de Investigaciones Científicas y Técnicas, Universidad de Buenos Aires, (J.A.B., P.V.P., M.E.G-C, J.T., C.V.R. E.K. and A.B.E.), Departamento de Fisiología, Biología Molecular y Celular, FCEyN, Universidad de Buenos Aires, Buenos Aires, Argentina (E.K.) and Department of Pharmacology, University College London, London, United Kingdom (S.K. and N.S.M.).

Molecular Pharmacology Fast Forward. Published on June 13, 2005 as DOI: 10.1124/mol.105.014431
This article has not been copyedited and formatted. The final version may differ from this version.

Running title: **block of α9α10 nicotinic receptors by quinolinic compounds**

Corresponding author:

Ana Belén Elgoyhen
Instituto de Investigaciones en Ingeniería Genética y Biología Molecular
(CONICET-UBA)
Vuelta de Obligado 2490
1428 Buenos Aires
Argentina

Fax: xx 5411 4 7868578
Phone: xx 5411 4 7832871
e-mail: elgoyhen@dna.uba.ar

number of text pages: 31

number of tables: 2

number of figures: 8

number of references: 39

words in Abstract: 202

words in Introduction: 514

words in Discussion: 1029

Abbreviations:

ACh: acetylcholine

BAPTA-AM: 1,2-bis(O-aminophenoxy)ethane-N,N,N',N'-tetraacetic acid

I-V: current-voltage relationship

MLA: methyllycaconitine

nAChRs: nicotinic acetylcholine receptors

Molecular Pharmacology Fast Forward. Published on June 13, 2005 as DOI: 10.1124/mol.105.014431
This article has not been copyedited and formatted. The final version may differ from this version.

ABSTRACT

In the present study, we report the effects of the quinoline derivatives, quinine, its optical isomer quinidine and chloroquine on α9α10-containing nicotinic cholinergic receptors (nAChRs). The compounds blocked acetylcholine (ACh)-evoked responses in α9α10-injected *Xenopus laevis* oocytes in a concentration-dependent manner, with a rank order of potency of: chloroquine (IC_{50}: 0.39 μM) > quinine (IC_{50}: 0.97 μM) ~ quinidine (IC_{50}: 1.37 μM). Moreover, chloroquine blocked ACh-evoked responses on rat cochlear inner hair cells with an IC_{50} value, 0.13 μM, within the same range as that observed for recombinant receptors. Block by chloroquine was purely competitive, whereas quinine inhibited ACh currents in a mixed competitive and noncompetitive manner. The competitive nature of the blockage produced by the three compounds was confirmed by equilibrium binding experiments using [^{3}H]-methyllycaconitine (MLA). Binding affinities (K_i values) were: 2.3, 5.5 and 13.0 μM for chloroquine, quinine and quinidine, respectively. Block by quinine was found to be only slightly voltage dependent, thus precluding open channel block as the main mechanism of interaction of quinine with α9α10 nAChRs. The present results add to the pharmacological characterization of α9α10-containing nicotinic receptors and indicate that the efferent olivocochlear system that innervates the cochlear hair cells is a target of these ototoxic antimalarial compounds.

Molecular Pharmacology Fast Forward. Published on June 13, 2005 as DOI: 10.1124/mol.105.014431
This article has not been copyedited and formatted. The final version may differ from this version.

Quinoline derivatives such as quinine, quinidine and chloroquine are well known for their use in the treatment of malaria. Its side effects on the auditory system have long been recognized and include reversible (but sometimes permanent) sensorineural hearing loss, tinnitus and vertigo (Jung et al., 1993). The mechanism of ototoxicity may involve different levels of the auditory system (Eggermont and Kenmochi, 1998; Jarboe and Hallworth, 1999). However, there is considerable evidence showing that the auditory periphery is the primary location underlying the reversible hearing loss induced by quinine (Lin et al., 1998; Puel et al., 1990). Perfusion of quinine into the perilymphatic space of guinea pig cochlea can result in a reduction of the compound action potential, cochlear microphonic and summating potential (Puel et al., 1990). In addition, it can affect the electromotility of outer hair cells (Zheng et al., 2001). Moreover, it can inhibit the K^+ current of outer hair cells and both the K^+ and Na^+ currents of the spiral ganglion cells (Lin et al., 1998), thus indicating a variety of effects of this compound on different ion channels.

It has been reported that quinine and quinidine can also block acetylcholine (ACh)–induced K^+ currents in outer hair cells and influence the effect of ACh on the compound action potential, suggesting a putative effect on the olivocochlear efferent system physiology (Daigneault et al., 1970; Yamamoto et al., 1997). Pharmacological and biophysical studies performed with the native cholinergic receptors present in mammalian and chicken hair cells (Fuchs, 1996) as well as cellular localization data (Elgoyhen et al., 1994; Elgoyhen et al., 2001; Lustig et al., 2001; Sgard et al., 2002) strongly suggest that the native receptor present at the efferent cholinergic olivocochlear-outer and developing inner hair cell synapse is assembled from both the $\alpha 9$ and $\alpha 10$

nicotinic subunits (Elgoyhen et al., 1994; Elgoyhen et al., 2001). Thus, α9α10-containing nicotinic cholinergic receptors (nAChRs) might be targets of the effects of quinoline compounds within the auditory system. In this regard, aminoglycosides, ototoxic drugs not related in structure with the quinoline compounds, have been reported as blockers of the α9α10 nAChRs (Rothlin et al., 2000), pinpointing this receptor as a possible site of interaction of ototoxic drugs. Moreover, the interaction of concentrations above 50 μM of quinine with nAChRs has been reported for receptors present at the neuromuscular junction, where it produces long-lived open-channel as well as a closed-channel block, and can normalize the open duration of channel events in the slow-channel congenital myasthenic syndrome (Fukudome et al., 1998; Sieb et al., 1996).

We have examined the effects of the quinoline derivatives quinine, quinidine and chloroquine (Fig. 1), on recombinant α9α10 nAChRs, reconstituted in *Xenopus laevis* oocytes. We show evidence that these compounds block the α9α10 nAChRs. The underlying mechanisms range from competitive in the case of chloroquine to mixed competitive and noncompetitive in the case of quinine. Moreover, we demonstrate that chloroquine blocks the native α9α10-containing nAChRs of inner hair cells. The present results indicate that the efferent olivocochlear system that innervates the cochlear hair cells is a direct target of these ototoxic antimalarial compounds.

Molecular Pharmacology Fast Forward. Published on June 13, 2005 as DOI: 10.1124/mol.105.014431
This article has not been copyedited and formatted. The final version may differ from this version.

MATERIALS AND METHODS

Expression of recombinant receptors in X. laevis oocytes

For expression studies, α9 and α10 rat nAChR subunits were subcloned into a modified pGEMHE vector (Liman et al., 1992). Capped cRNAs were *in vitro* transcribed from linearized plasmid DNA templates using the mMessage mMachine T7 Transcription Kit (Ambion Corporation, Austin, TX). The maintenance of *X. laevis* as well as the preparation and cRNA injection of stage V and VI oocytes has been described in detail elsewhere (Katz et al., 2000). Typically, oocytes were injected with 50 nl of RNase-free water containing 0.01 - 1.0 ng of cRNAs (at a 1:1 molar ratio) and maintained in Barth's solution at 17° C.

Electrophysiological recordings were performed 2-6 days after cRNA injection under two-electrode voltage-clamp with a Geneclamp 500 amplifier (Axon Instruments Corp., Union City, CA). Both voltage and current electrodes were filled with 3 M KCl and had resistances of ~1-2 MΩ. Data acquisition was performed using a Digidata 1200 and the pClamp 7.0 software (Axon Instruments Corp., Union City, CA). Data were analyzed using Clamp Fit from the pClamp 6.1 software. During electrophysiological recordings, oocytes were continuously superfused (~10 ml/min) with normal frog saline comprised of (mM): 115 NaCl, 2.5 KCl, 1.8 $CaCl_2$, and 10 HEPES buffer, pH 7.2. Unless otherwise indicated, the membrane potential was clamped to -70 mV. Drugs were applied in the perfusion solution of the oocyte chamber. To minimize activation of the endogenous Ca^{2+}-sensitive chloride current (Elgoyhen et al., 2001), all experiments were performed in oocytes incubated with the Ca^{2+} chelator 1,2-bis(2-aminophenoxy)ethane-

Molecular Pharmacology Fast Forward. Published on June 13, 2005 as DOI: 10.1124/mol.105.014431
This article has not been copyedited and formatted. The final version may differ from this version.

N,*N*,*N'*,*N'*-tetraacetic acid-acetoxymethyl ester (BAPTA-AM, 100 μM) for 3-4 hr prior to electrophysiological recordings.

Concentration-response curves were normalized to the maximal agonist response in each oocyte. For the inhibition curves, antagonists were added to the perfusion solution for 2 min prior to the addition of 10 μM ACh and then were co-applied with this agonist. Responses were referred to as a percentage of the response to ACh. The mean and standard error of the mean of peak current responses are represented. Agonist concentration-response curves were iteratively fitted with the equation:

$$I/I_{max} = A^n / (A^n + EC_{50}^n), \text{ (Eq. 1)},$$

where I is the peak inward current evoked by agonist at concentration A; I_{max} is current evoked by the concentration of agonist eliciting a maximal response; EC_{50} is the concentration of agonist inducing half-maximal current response and n is the Hill coefficient. An equation of the same form was used to analyze the concentration dependency of antagonist-induced blockage. The parameters derived were the concentration of antagonist producing a 50% block of the control response to ACh (IC_{50}) and the associated interaction coefficient (n). Analysis of competitive inhibition was performed by the Schild plot (Arunlakshana and Schild, 1959), with the following equation:

$$\log [(A'/A)-1] = \log B - \log K_B, \text{ (Eq. 2)},$$

where A and A' are the EC_{50} of ACh in the absence and presence of antagonist, respectively, B is the concentration of antagonist and K_B is the equilibrium dissociation constant for the combination of the antagonist with the receptor. Further analysis was performed using the Gaddum-Schild equation as recommended (Neubig et al., 2003):

Molecular Pharmacology Fast Forward. Published on June 13, 2005 as DOI: 10.1124/mol.105.014431
This article has not been copyedited and formatted. The final version may differ from this version.

$$pEC_{50} = -\log([B]^S + 10^{-pA_2 S}) - \log c, \text{ (Eq. 3)},$$

where pEC_{50} is the negative logarithm of the EC_{50} of the agonist, pA_2 the negative logarithm of the molar concentration of the antagonist that makes it necessary to double the concentration of the agonist needed to elicit the original response obtained in the absence of antagonist, [B] the antagonist concentration, S the logistic slope factor and log c a fitting constant. When S equals 1, pA2 corresponds to the negative logarithm of K_B. The analysis of the correlation of IC_{50} values as a function of the concentration of agonist was performed by the Cheng-Prusoff equation (Cheng and Prusoff, 1973), with the modification introduced by Leff and Dougall (Leff and Dougall, 1993):

$$IC_{50} = K_B[(2+\{A/EC_{50}\}^n)^{1/n}]-1, \text{ (Eq. 4)},$$

where n is the Hill coefficient, A is the agonist concentration and other parameters have already been defined.

Current-voltage (I-V) relationships were obtained by applying 2 sec voltage ramps from +50 to -120 mV, 5 seconds after the peak response to ACh from a holding potential of –70 mV. Leakage correction was performed by digital subtraction of the I-V curve obtained by the same voltage ramp protocol prior to the application of ACh. Generation of voltage protocols and data acquisition were performed using a Digidata 1200 and the pClamp 6.1 or 7.0 software (Axon Instruments Corp., Union City, CA). Data were analyzed using Clamp fit from the pClamp 6.1 software.

Electrophysiological recordings from hair cells

Apical turns of the organ of Corti were excised from Sprague-Dawley rats at postnatal ages P9-11 and used within 3 hours. Day of birth was considered postnatal day

Molecular Pharmacology Fast Forward. Published on June 13, 2005 as DOI: 10.1124/mol.105.014431
This article has not been copyedited and formatted. The final version may differ from this version.

0, P0. Cochlear preparations were mounted under an Axioskope microscope (Zeiss, Oberkochem, Germany) and viewed with differential interference contrast (DIC) using a 63x water immersion objective and a camera with contrast enhancement (Hamamatsu C2400-07, Hamamatsu City, Japan). Methods to record from IHCs were essentially as described previously (Glowatzki and Fuchs, 2000; Katz et al., 2004).

Briefly, inner hair cells were identified visually with the 63x objective and during recordings, by the size of their capacitance (7 to 12 pF), by their characteristic voltage-dependent Na^+ and K^+ currents, and at older ages including a fast-activating K^+-conductance (Kros et al., 1998). Some cells were removed to access the inner hair cells, but mostly the pipette moved through the tissue under positive pressure. The extracellular solution was as follows (in mM): 155 NaCl, 5.8 KCl, 1.3 $CaCl_2$, 0.9 $MgCl_2$, 0.7 NaH_2PO_4, 5.6 D-glucose, and 10 Hepes buffer; pH 7.4. The pipette solution contained (in mM): 150 KCl, 3.5 $MgCl_2$, 0.1 $CaCl_2$, 5 1,2-bis(2-aminophenoxy)ethane-N,N,N´,N´-tetraacetic acid (BAPTA) buffer, 2.5 Na_2ATP, pH 7.2. In order to minimize even more the contribution of small conductance Ca^{2+}-activated K^+, in addition to using BAPTA in the pipette solution, the K^+ channel blocker apamin (1 nM) was added to the external working solutions. Glass pipettes, 1.2 mm I.D, had resistances of 7-10 MΩ. Experiments were done at a holding voltage of –90 mV and all working solutions were made up in a saline containing only 0.5 mM Ca^{2+} and no Mg^{2+} so as to optimize the experimental conditions for measuring currents flowing through the α9α10 receptors (Katz et.al., 2004; Weisstaub et al., 2002).

Solutions were applied by a gravity-fed multichannel glass pipette (~150 μM tip diameter), positioned about 300 μM from the recorded cell. Currents were recorded in the

Molecular Pharmacology Fast Forward. Published on June 13, 2005 as DOI: 10.1124/mol.105.014431
This article has not been copyedited and formatted. The final version may differ from this version.

whole-cell patch-clamp mode with an Axopatch 200B amplifier, low-pass filtered at 2-10 kHz and digitized at 5-20 kHz with a Digidata 1200 board (Axon Instruments Corp., Union City, California). Recordings were made at room temperature (22-25 ºC). Holding potentials were not corrected for liquid junction potentials or for the voltage drop across the uncompensated series resistance.

Mammalian cell culture and transfection

Mammalian cell line, tsA201, derived from the human embryonic kidney HEK293 cell line, were cultured in Dulbecco's modified Eagle's medium (Gibco Invitrogen, Paisley, UK) containing 2 mM L-Glutamax™ (Gibco Invitrogen, Paisley, UK) plus 10% heat-inactivated fetal calf serum (Sigma, Poole, UK), with penicillin (100 U/ml) and streptomycin (100 μg/ml) and were maintained in a humidified incubator containing 5% CO_2 at 37°C. Cells were cotransfected with pRK5-$\alpha9^{(L209)}$/$5HT_{3A}$ and pRK5-$\alpha10^{(L206)}$/$5HT_{3A}$ (Baker et al., 2004) using Effectene™ transfection reagent (Qiagen, Crawley, UK) according to the manufacturer's instructions. Cells were transfected overnight and assayed for expression approximately 40-48 hours after transfection.

Radioligand Binding

Binding studies with [^{3}H]methyllycaconitine ([^{3}H]MLA; Tocris Cookson Ltd, Avonmouth, UK; specific activity 26 Ci/mmol) to cell membrane preparations were performed, essentially as described previously (Baker and Millar, 2004). Membranes (typically 80-150 μg protein) were incubated with radioligand for 150 min at 4°C in a

Molecular Pharmacology Fast Forward. Published on June 13, 2005 as DOI: 10.1124/mol.105.014431
This article has not been copyedited and formatted. The final version may differ from this version.

total volume of 150 µl in the presence of protease inhibitors leupeptin (2 µg/ml) and pepstatin (1 µg/ml). Radioligand binding was assayed by filtration onto Whatman GF/B filters (pre-soaked in 0.5% polyethylenimine), followed by rapid washing with cold 10 mM phosphate buffer using a Brandel cell harvester. Bound radioligand was quantified by scintillation counting. Curves for equilibrium binding were fitted with the Hill equation by equally-weighted least-squares (CVFIT program, David Colquhoun, University College London). IC_{50} values were converted to Ki values by applying the Cheng-Prusoff correction.

Statistical Analysis

Statistical significance was evaluated by the Student's *t* test (two-tailed, unpaired samples). Multiple comparisons of IC_{50} values were performed with a one-way ANOVA followed by Tukey's test. A $p<0.05$ was considered significant.

Materials

ACh chloride, quinine hemisulfate, quinidine chloride and chloroquine diphosphate were bought from Sigma Chemical Co. (St. Louis, MO). BAPTA-AM (Molecular Probes, Eugene, OR) was stored at –20 °C as aliquots of a 100 mM solution in dimethyl sulfoxide, thawed and diluted 1000-fold into saline solution shortly before incubation of the oocytes.

Molecular Pharmacology Fast Forward. Published on June 13, 2005 as DOI: 10.1124/mol.105.014431
This article has not been copyedited and formatted. The final version may differ from this version.

All experimental protocols were carried out in accordance with the National Institute of Health guide for the care and use of Laboratory animals (NIH Publications No. 80-23) revised 1978.

RESULTS

Effect of antimalarial quinoline derivatives on the α9α10 recombinant nAChR.

Figure 2 A shows representative responses to 10 μM ACh (i.e. a concentration close to the one that produces a half-maximal response, EC_{50}, Elgoyhen et al., 2001) of *X. laevis* oocytes injected with α9 and α10 cRNAs, and block of these responses in the presence of either quinine, quinidine and chloroquine at a membrane potential of -70 mV. The amplitude of the ACh responses was markedly reduced at micromolar concentrations of the quinoline derivatives. In order to evaluate the potency of the compounds, inhibition curves were carried out (Fig. 2 B). Currents evoked by ACh were blocked in a concentration-dependent manner with a rank order of potency of chloroquine (IC_{50}: 0.39±0.08 μM, Hill coefficient: 1.2±0.1, n=6) > quinine (IC_{50}: 0.97±0.07 μM, Hill coefficient: 1.37±0.29, n=6) ~ quinidine (IC_{50}: 1.28±0.05 μM, Hill coefficient: 1.2±0.1, n=6), $p < 0.05$. Block by antagonists was reversible, because initial control responses to ACh were recovered after washes of the oocytes with frog saline for 3 minutes. Moreover, antagonists did not elicit *per se* responses in oocytes expressing α9α10 receptors.

Underlying mechanisms of block.

Molecular Pharmacology Fast Forward. Published on June 13, 2005 as DOI: 10.1124/mol.105.014431
This article has not been copyedited and formatted. The final version may differ from this version.

The mechanism underlying the blocking action of chloroquine, quinine and quinidine on the α9α10 receptor was further analyzed on recombinant receptors. Thus concentration-response curves to ACh were performed in the absence or presence of the different antagonists (Fig. 3). At 1μM, both quinine (Fig. 3 A) as well as quinidine (Fig. 3 B) shifted the concentration-response curves to ACh to higher concentrations without altering its maximal response, a behavior typical of a competitive antagonist. At higher concentrations of the antagonists, however, the maximal evoked ACh response was reduced (Figs 3 A and B; Table 1), indicating an additional effect. A shift to the right in the concentration-response curve, with concomitant unsurmountable antagonistic effects at high concentrations of the agonist, is indicative of a noncompetitive inhibition. In contrast, chloroquine produced parallel rightward shifts in the ACh concentration-response curves with increases in the EC_{50}. Moreover, it seemed to be a purely competitive antagonist, because full recovery of maximal ACh responses could be obtained even in the presence of a 10 μM concentration, which is 26-fold higher than its IC_{50} value (Fig. 3 C and Table 2). Higher concentrations of chloroquine could not be tested, since the degree of block was so high that desensitizing millimolar concentrations of ACh would have been needed to overcome the blocking effect. The competitive nature of the blockage by chloroquine was further tested performing a Schild plot (Eq. 2, Fig. 4 A). The linear regression analysis gave rise to a straight line of almost unit slope (0.97±0.19, r^2= 0.93), thus confirming the competitive nature of the antagonism. The intersection on the x axes gave an estimated equilibrium dissociation constant for the combination of the antagonist with its interacting site (K_B) of 0.35 μM. In addition, if a non-linear regression analysis is used to fit agonist/antagonist concentration-response

Molecular Pharmacology Fast Forward. Published on June 13, 2005 as DOI: 10.1124/mol.105.014431
This article has not been copyedited and formatted. The final version may differ from this version.

data to the Gaddum-Schild equation (Eq. 3), as recommended by Neubig et al. (2003), the logistic slope factor S was again near unity, 0.98 ± 0.05, r^2= 0.99 and a similar K_B, 0.33 μM, was obtained (Fig. 4 inset).

In order to further examine the noncompetitive interaction of quinine, we co-applied increasing concentrations of this antagonist with different concentrations of ACh (ranging from 5 to 300 μM), obtaining the respective inhibition curves and subsequently plotted the IC_{50} values as a function of the concentration of ACh (Fig. 5 A and inset). The same analysis was performed with chloroquine, to compare the results of quinine with those of a pure competitive antagonist (Fig. 5 B and inset). As expected, IC_{50} values for the antagonists increased when the ACh concentration was increased, and full inhibition was observed at high concentrations of the antagonists. The data from these experiments were then used and compared to the fit performed by the Cheng-Prusoff equation (Cheng and Prusoff, 1973), with the modification introduced by Leff and Dougall, Eq.4 in methods (Leff and Dougall, 1993). This equation predicts the IC_{50} values at a given concentration of agonist for a competitive antagonist of allosteric receptors. The theoretical curves where drawn using an EC_{50} value for ACh of 13 μM, a Hill coefficient of 1.2 derived from ACh concentration-response curves (Fig. 3 and Elgoyhen et al., 2001), and a K_B of 0.73 μM for quinine (calculated using the Leff-Dougall Eq. 4 for an IC_{50} of 0.97 μM derived from Fig. 2 B) and 0.39 μM for chloroquine (derived from data in Fig. 2 B). As observed in Fig. 5 A, in the case of quinine the experimental IC_{50} values adjusted to the theoretical curve at concentrations below 100 μM ACh, thus suggesting competitive inhibition. At higher concentrations of ACh, the experimental values deviated from those estimated by the equation, thus confirming additional

Molecular Pharmacology Fast Forward. Published on June 13, 2005 as DOI: 10.1124/mol.105.014431
This article has not been copyedited and formatted. The final version may differ from this version.

noncompetitive block by quinine. On the other hand, in the case of chloroquine all experimental data fitted the equation, thus confirming the competitive nature of this antagonist (Fig. 5 B). Moreover, the same K_B value as derived from the Schild analysis was obtained.

Since quinine is a positively charged molecule at physiological pH, an interaction with the pore of the channel could account for the noncompetitive type of block. If this were the case, then the blockage should be reduced at depolarized when compared to hyperpolarized potentials. In order to evaluate the voltage-dependency of the quinine block, 2-sec voltage ramp protocols (+50 to -120 mV) were performed in the presence of 300 μM ACh either alone or co-applied with quinine 10 μM. As shown in the representative I–V curves in Fig. 6 A, blockage by quinine was more pronounced at hyperpolarized potentials. Fig. 6 B was performed with the current amplitude values derived from I–V curves like the one shown in Fig. 6 A. Block by quinine was dependent upon the membrane holding potential, being significantly larger at hyperpolarized than at depolarized holding potentials (I/Imax: 0.13±0.02 and 0.35±0.05 at -120 and +50 mV respectively, $p<0.05$, $n=7$). However, an *e*-fold difference in I/Imax was only attained every 160 mV, thus indicating only a slight dependence upon membrane potential.

Competition binding data with chloroquine, quinine and quinidine

Competition radioligand binding was used to examine whether chloroquine, quinine and quinidine were able to displace binding of the high affinity nicotinic antagonist methyllycaconitine. Experiments were performed in transfected tsA201 cells using subunit chimeras ($\alpha9^{(L209)}/5HT_{3A}$ and $\alpha10^{(L206)}/5HT_{3A}$) in which the extracellular

Molecular Pharmacology Fast Forward. Published on June 13, 2005 as DOI: 10.1124/mol.105.014431
This article has not been copyedited and formatted. The final version may differ from this version.

N-terminal domain of the α9 or α10 subunits were fused to the transmembrane and intracellular domain of the mouse $5HT_{3A}$ subunit (Baker et al., 2004). These chimeric receptors express very well in transfected cells (compared to wild-type α9α10 receptors), binding experiments give a good specific to non-specific signals, and chimeric receptors retain the same pharmacological profile when compared to wild-type receptors expressed in *X. laevis* oocytes. As described previously, [^{3}H]MLA binds with high affinity (K_d = 7.5±1.2 nM) to cells co-expressing the α9 and α10 subunit chimeras (Baker et al., 2004). Equilibrium competition binding studies were performed with chloroquine, quinine and quinidine to determine their affinity for α9α10 receptors (Fig. 7). In all cases, complete displacement of bound [^{3}H]MLA was observed, providing evidence of competitive binding to a single high affinity site. Binding affinities (K_i values) determined from three independent experiments were: chloroquine, 2.3±0.5 μM, quinine, 5.5±0.7 μM and quinidine, 13.0±2.9 μM. Thus the rank order of potency was similar as that obtained from functional data in *X. laevis* oocytes.

Chloroquine blocks native α9α10-containing nAChRs of rat cochlear inner hair cells.

It is currently accepted that olivocochlear efferent innervation to developing inner hair cells is subserved by a nAChR composed from both α9 and α10 nicotinic subunits (Elgoyhen et al., 2001; Katz et al., 2004; Lustig et al., 2001, Fuchs 1996). We therefore studied the effects of chloroquine, the most potent blocking agent, on ACh responses (measured in isolation from the small conductance Ca^{2+}-activated K^+ channels) in inner hair cells from acutely excised organs of Corti of P9-11 rats, as a source of native receptors. As shown on the representative traces of Fig. 8 A and on the concentration-

Molecular Pharmacology Fast Forward. Published on June 13, 2005 as DOI: 10.1124/mol.105.014431
This article has not been copyedited and formatted. The final version may differ from this version.

response curves of Fig. 8 B, similar to that described for recombinant α9α10 receptors, chloroquine blocked responses to 60 μM ACh (the EC_{50} in this system, Katz et.al., 2004) with an IC_{50} of 0.13±0.01 μM, n= 5.

DISCUSSION

In the present study we analyzed the effects of the quinoline compounds quinine, its optical isomer quinidine and chloroquine on the recombinant α9α10 nAChR expressed in *X. laevis* oocytes. We report based on functional data that, whereas quinine and quinidine blocked ACh responses through a mixed competitive and noncompetitive mechanism, chloroquine blocked the receptors through a competitive mechanism. The competitive nature of the block produced by the three compounds was verified by ligand-binding experiments. Moreover, in the case of chloroquine the blocking action was also observed on native α9α10-containing receptors of rat cochlear inner hair cells.

The observation that block by chloroquine was purely competitive is indicating that this compound shares with ACh at least part of the binding pocket, in such a way that occupancy of the site is mutually exclusive. ACh and all other agonists and competitive antagonists contain a positively charged quarternary ammonium group or a tertiary nitrogen group that can be protonated and that interacts with electron rich side chains of aromatic residues within the nAChRs (Karlin, 2002). In this regard, chloroquine, quinine and quinidine fulfill these criteria (Fig. 1). Although a structure-function study is beyond the scope of this work, the fact that quinine and quinidine produced an additional noncompetitive mechanism of block, should derive from the fact that different to chloroquine, these compounds have a quinuclidine ring (Fig. 1) attached to the quinoline

Molecular Pharmacology Fast Forward. Published on June 13, 2005 as DOI: 10.1124/mol.105.014431
This article has not been copyedited and formatted. The final version may differ from this version.

moiety (Tracy and Webster Jr, 2001). This might generate an additional site of interaction with the receptor.

If the interaction of quinine with the α9α10 nAChR requires the entrance into the transmembrane field, then depolarization should reduce inhibition. The simplest explanation for a voltage-dependent block is that the blocking molecule either has a binding site within the channel, partway across the electric field of the membrane (i.e. an open channel blocker) or that it docks within the channel vestibule impairing ion flow. However, as derived from Fig. 6, an approximate *e*-fold difference in I/I_{max} was achieved every 160 mV. This indicates that blockage by quinine was only slightly dependent on the membrane potential and could imply that the blocker binds very near to the entrance of the pore. In this regard, it has been reported that quinine, quinidine and chloroquine also block muscle type nAChRs. Patch clamp recordings have demonstrated that quinine at micromolar concentrations produces a long-lived open-channel as well as a closed-channel block of muscle nAChRs (Sieb et al., 1996). Similar mechanisms could account for the effects of this drug on α9α10 nAChRs. However, complete analysis at the single channel level, which so far have been difficult to achieve in α9α10-expressing cells (Plazas et al., 2005), would be necessary to define the underlying mechanism of block.

Quinoline derivatives have a variety of effects on several cochlear hair cell K^+ currents. Thus quinine blocks voltage-dependent K^+ currents in isolated outer hair cells of the guinea pig (Lin et al., 1995). Moreover, it has been proposed that both quinine and quinidine block the small conductance Ca^{2+}-activated K^+ channels of guinea pig outer hair cells (Yamamoto et al., 1997). Current data supports the notion that the inhibitory nature of the cholinergic olivocochlear synapse in both outer and inner hair cells is

Molecular Pharmacology Fast Forward. Published on June 13, 2005 as DOI: 10.1124/mol.105.014431
This article has not been copyedited and formatted. The final version may differ from this version.

caused by the activation of a small conductance Ca^{2+}-activated K^+ current after Ca^{2+} influx through the α9α10-containing nicotinic receptors (Elgoyhen et al., 2001; Fuchs 1996). The present results show that chloroquine blocks both native and recombinant α9α10-containing nAChRs, thus indicating that quinoline derivatives are direct blockers of the nAChR rather than of the small conductance Ca^{2+}-activated K^+ channels as suggested by Yamamoto et al. (1997). Although non-selective for α9α10 nAChRs, the IC_{50} values obtained for the quinoline derivatives at 10 μM ACh are similar to those obtained for atropine, nicotine, d-tubocurarine and bicuculline (Elgoyhen et al., 2001). Thus, quinoline derivatives can be used as tools to further define the pharmacological profile of these receptors.

Clinical implications

Quinoline derivatives cause a substantial but usually reversible sensorineural hearing loss at middle to high frequencies accompanied by tinnitus and vertigo (Jung et al., 1993). The mechanism of ototoxicity may involve different levels of the auditory system (Eggermont and Kenmochi, 1998; Jarboe and Hallworth, 1999). However, there is considerable evidence showing that the auditory periphery is the primary location underlying the hearing loss induced by quinine (Lin et al., 1998; Puel et al., 1990). Both a direct action of quinine on the spiral ganglion neurons and/or their synaptic terminals to the inner hair cells as well as on the outer hair cell electromotility have been proposed as underlying mechanisms for the ototoxicity (Berninger et al., 1998; McFadden and Pasanen, 1994; Zheng et al., 2001). Outer hair cell activity is under the direct control of the efferent cholinergic olivocochlear fibers, through the release of ACh and the

Molecular Pharmacology Fast Forward. Published on June 13, 2005 as DOI: 10.1124/mol.105.014431
This article has not been copyedited and formatted. The final version may differ from this version.

subsequent activation of α9α10-containing nAChRs (Elgoyhen et al., 2001; Guinan, 1996). The results we present in the present work further indicate that these nAChRs are also the target of the quinoline derivatives and therefore that this effect could eventually contribute to the ototoxicity produced by these compounds. In this regard, it has been shown that chloroquine increases the sensitivity to noise induced trauma (Barrenas and Holgers, 2000). Since the efferent system protects the inner ear against noise induced trauma (Patuzzi and Thompson, 1991), block of the system in the presence of chloroquine could account for the above described increased damage.

Humans receiving treatment with quinoline derivatives can attain plasmatic drug levels within the range in which they block the α9α10 nAChR. Thus, in patients with cardiac arrhythmias and malaria, the therapeutic plasma concentrations of quinine and quinidine fall within the micromolar range (Franke et al., 1983; Kessler et al., 1974). Quinine is also used as a flavoring agent in tonic water and some liquors (Worner et al., 1989). In the United States and Germany, federal regulations limit the amount of quinine in carbonated beverages to 83 mg/l and 85 mg/l, respectively. However, the daily consumption of 105 mg quinine in tonic water for two weeks leads to a serum level of about 0.7 μM (Zajtchuk et al., 1984). Clearly, the quinoline derivatives must be used with caution when the safety margin of the auditory system is already compromised.

Molecular Pharmacology Fast Forward. Published on June 13, 2005 as DOI: 10.1124/mol.105.014431
This article has not been copyedited and formatted. The final version may differ from this version.

REFERENCES

Arunlakshana O and Schild HO (1959) Some quantitative uses of drug antagonists. *Br J Pharmacol* **14**:48-58.

Baker ER, Zwart R, Sher E and Millar NS (2004) Pharmacological properties of alpha 9 alpha 10 nicotinic acetylcholine receptors revealed by heterologous expression of subunit chimeras. *Mol Pharmacol* **65**:453-460.

Barrenas ML and Holgers KM (2000) Ototoxic interaction between noise and pheomelanin: distortion product otoacoustic emissions after acoustical trauma in chloroquine-treated red, black, and albino guinea pigs. *Audiology* **39**:238-246.

Berninger E, Karlsson K and Alvan G (1998) Quinine reduces the dynamic range of the human auditory system. *Acta Otolaryngol* **118**:46-51.

Cheng Y and Prusoff WH (1973) Relationship between the inhibition constant (K1) and the concentration of inhibitor which causes 50 per cent inhibition (I50) of an enzymatic reaction. *Biochem Pharmacol* **22**:3099-3108.

Daigneault EA, Pruett JR and Brown RD (1970) Influence of ototoxic drugs on acetylcholine-induced depression of the cochlear N1 potential. *Toxicol Appl Pharmacol* **17**:223-230.

Eggermont JJ and Kenmochi M (1998) Salicylate and quinine selectively increase spontaneous firing rates in secondary auditory cortex. *Hear Res* **117**:149-160.

Elgoyhen AB, Johnson DS, Boulter J, Vetter DE and Heinemann S (1994) α9: an acetylcholine receptor with novel pharmacological properties expressed in rat cochlear hair cells. *Cell* **79**:705-715.

Elgoyhen AB, Vetter D, Katz E, Rothlin C, Heinemann S and Boulter J (2001) Alpha 10: A determinant of nicotinic cholinergic receptor function in mammalian vestibular and cochlear mechanosensory hair cells. *Proc Nat Acad Sci, USA* **98**:3501-3506.

Franke U, Proksch B, Muller M, Risler M and Ehninger G (1983) Drug monitoring of quinine by HPLC in cerebral malaria with acute renal failure treated by haemofiltration. *Eur J Clin Pharmacol* **15**:345-350.

Fuchs P (1996) Synaptic transmission at vertebrate hair cells. *Current Opinion in Neurobiol.* **6**:514-519.

Fukudome T, Ohno K, Brengman JM and Engel AG (1998) Quinidine normalizes the open duration of slow-channel mutants of the acetylcholine receptor. *Neuroreport* **9**:1907-1911.

Guinan JJ (1996) Physiology of olivocochlear efferents, in *The Cochlea* (Dallos, Popper and Fay eds) pp 435-502, Springer-Verlag, New York.

Jarboe JK and Hallworth R (1999) The effect of quinine on outer hair cell shape, compliance and force. *Hear Res* **132**:43-50.

Jung TT, Rhee CK, Lee CS, Park YS and Choi DC (1993) Ototoxicity of salicylate, nonsteroidal antiinflammatory drugs, and quinine. *Otolaryngol Clin North Am* **26**:791-810.

Karlin A (2002) Ion channel structure: emerging structure of the nicotinic acetylcholine receptors. *Nature Reviews Neurosc* **3**:102-114.

Katz E, Elgoyhen AB, Gomez-Casati ME, Knipper M, Vetter DE, Fuchs PA and Glowatzki E (2004) Developmental regulation of nicotinic synapses on cochlear inner hair cells. *J Neurosci* **24**:7814-7820.

Katz E, Verbitsky M, Rothlin C, Vetter D, Heinemann S and Elgoyhen A (2000) High calcium permeability and calcium block of the α9 nicotinic acetylcholine receptor. *Hearing Res* **141**:117-128.

Kessler K, Lowenthal D, Warner H, Gibson T, Briggs W and Reidenberg M (1974) Quinidine elimination in patients with congestive heart failure or poor renal function. *New Engl J Med* **290**:706-709.

Kros CJ, Ruppersberg JP and Rusch A (1998) Expression of a potassium current in inner hair cells during development of hearing in mice. *Nature* **394**:281-284.

Leff P and Dougall IG (1993) Further concerns over Cheng-Prusoff analysis. *Trends Pharmacol Sci* **14**:110-112.

Liman ER, Tytgat J and Hess P (1992) Subunit stoichiometry of a mammalian K+ channel determined by construction of multimeric cDNAs. *Neuron* **9**:861-871.

Lin X, Chen S and Tee D (1998) Effects of quinine on the excitability and voltage-dependent currents of isolated spiral ganglion neurons in culture. *J Neurophysiol* **79**:2503-2512.

Lin X, Hume R and Nuttall A (1995) Dihydropyridines and verapamil inhibit voltage-dependent K^+ current in isolated outer hair cells of the guinea pig. *Hearing Res* **88**:36-46.

Lustig LR, Peng H, Hiel H, Yamamoto T and Fuchs P (2001) Molecular cloning and mapping of the human nicotinic acetylcholine receptor α10 (CHRNA10). *Genomics* **73**:272-283.

McFadden D and Pasanen E (1994) Otoacustic emissions and quinine sulfate. *J Acoust Soc Am* **95**:3460-3474.

Neubig RR, Spedding M, Kenakin T and Christopoulos A (2003) International Union of Pharmacology Committee on Receptor Nomenclature and Drug Classification. XXXVIII. Update on terms and symbols in quantitative pharmacology. *Pharmacol Rev* **55**:597-606.

Patuzzi RB and Thompson ML (1991) Cochlear efferent neurons and protection against acoustic trauma: Protection of outer hair cell receptor current and interanimal variability. *Hearing Res.* **54**:45-58.

Plazas PV, De Rosa MJ, Gomez-Casati ME, Verbitsky M, Weisstaub N, Katz E, Bouzat C and Elgoyhen AB (2005) Key roles of hydrophobic rings of TM2 in gating of the alpha9alpha10 nicotinic cholinergic receptor. *Br J Pharmacol, in press.*

Puel JL, Bobbin RP and Fallon M (1990) Salicylate, mefenamate, meclofenamate, and quinine on cochlear potentials. *Otolaryngol Head Neck Surg* **102**:66-73.

Rothlin CV, Katz E, Verbitsky M, Vetter D, Heinemann S and Elgoyhen AB (2000) Block of the α9 nicotinic receptor by ototoxic aminoglycosides. *Neuropharmacology* **39**:2525-2532.

Sgard F, Charpentier E, Bertrand S, Walker N, Caput D, Graham D, Bertrand D and Besnard F (2002) A novel human nicotinic receptor subunit, α10, that confers functionality to the α9-subunit. *Molec Pharmacol* **61**:150-159.

Sieb JP, Milone M and Engel AG (1996) Effects of the quinoline derivatives quinine, quinidine, and chloroquine on neuromuscular transmission. *Brain Res* **712**:179-189.

Tracy J and Webster Jr L (2001) Chemotherapy of parasitic infections, in *Goodman &Gilman´s The Pharmacological Basis of Therapeutics* (Hardman LGG ed) pp 1059-1120, McGraw-Hill.

Weisstaub N, Vetter D, Elgoyhen A and Katz E (2002) The alpha9/alpha10 nicotinic acetylcholine receptor is permeable to and is modulated by divalent cations. *Hearing Res* **167**: 122-135.

Worner M, Gensler M, Bahn B and Schreier P (1989) Use of solid phase extraction for rapid sample preparation in the determination of food constituents. I. Quinine in beverages. *Z Lebensm Unters Forsch* **189**:422-425.

Yamamoto T, Kakehata S, Yamada T, Saito T, Saito H and Akaike N (1997) Effects of potassium channel blockers on the acetylcholine-induced currents in dissociated outer hair cells of guinea pig cochlea. *Neurosci Lett* **236**:79-82.

Zajtchuk JT, Mihail R, Jewell JS, Dunne MJ and Chadwick SG (1984) Electronystagmographic findings in long-term low-dose quinine ingestion. A preliminary report. *Arch Otolaryngol* **110**:788-791.

Zheng J, Ren T, Parthasarathi A and Nuttall AL (2001) Quinine-induced alterations of electrically evoked otoacoustic emissions and cochlear potentials in guinea pigs. *Hear Res* **154**:124-34.

Molecular Pharmacology Fast Forward. Published on June 13, 2005 as DOI: 10.1124/mol.105.014431
This article has not been copyedited and formatted. The final version may differ from this version.

FOOTNOTES

This work was supported by an International Research Scholar grant from the Howard Hughes Medical Institute, the Agencia Nacional de Promoción Científica y Tecnológica, the University of Buenos Aires (A.B.E.) and the Welcome Trust (N.S.M.) J.A.B. is supported by an undergraduate fellowship from the University of Buenos Aires, P.V.P. and M.E.G-C by a CONICET predoctoral fellowship, J.T. by a fellowship from ANPCyT and S.K. by a Welcome Trust studentship in Neuroscience.

C.V.R. present address: The Salk Institute for Biological Studies, La Jolla, CA, 92037.

Person to receive reprint requests:

Ana Belén Elgoyhen

Instituto de Investigaciones en Ingeniería Genética y Biología Molecular

(CONICET-UBA)

Vuelta de Obligado 2490

1428 Buenos Aires

Argentina

Fax: xx 5411 4 7868578

Phone: xx 5411 4 7832871

e-mail: elgoyhen@dna.uba.ar

Molecular Pharmacology Fast Forward. Published on June 13, 2005 as DOI: 10.1124/mol.105.014431
This article has not been copyedited and formatted. The final version may differ from this version.

Fig. 1. Chemical structures of quinine, quinidine and chloroquine.

Fig. 2. Effect of quinoline drivatives on ACh-evoked currents through recombinant α9α10 nAChRs. A, representative traces to ACh either alone or in the presence of quinine, quinidine or chloroquine. B, inhibition curves performed by the co-application of 10 μM ACh and increasing concentrations of the compounds. Oocytes were incubated with each concentration of the antagonists for 2 min prior to the addition of ACh. Peak current values are plotted, expressed as the percentage of the peak control current evoked by ACh. The mean and S.E.M. of six experiments per group are shown.

Fig. 3. Mechanism of blockage of ACh-evoked responses by quinoline derivatives. A, concentration-response curves to ACh performed either alone (■) or in the presence of 1 μM (▲), 3 μM (□) or 10 μM (▼) quinine. B, same experiment as in A, but in the presence of quinidine. C, same as in A, but in the presence of 0.3 μM (○), 1 μM (▲), 5 μM (●) or 10 μM (▼) chloroquine. Peak current values were normalized and referred to the maximal peak response to ACh. The mean and S.E.M. of four to twelve experiments per group are shown.

Fig. 4. Competitive block of ACh responses by chloroquine. A, Schild plot (Eq. 2) performed with data derived from Fig 3. Note that the slope is near unity and that the K_B derived from the intercept to the x axis is 0.35 μM. B, Gaddum-Schild plot (Eq. 3) performed with data derived from Fig 3. Note that the logistic slope factor is near unity and that the estimated K_B is 0.33 μM.

Molecular Pharmacology Fast Forward. Published on June 13, 2005 as DOI: 10.1124/mol.105.014431
This article has not been copyedited and formatted. The final version may differ from this version.

Fig. 5. Inhibition curves at different ACh concentrations. A, Inhibition curves performed at increasing concentrations of quinine and either 5 μM (○), 10 μM (■), 15 μM (×), 30 μM (◊), 50 μM (▼), 100 μM (▲), 200 μM (♦) or 300 μM (●) ACh. Oocytes were incubated with each concentration of the antagonists for 2 min prior to the addition of ACh. Peak current values are plotted, expressed as the percentage of the peak control current evoked by ACh. B, Same experiment as in A but with increasing concentrations of chloroquine and either 5 μM (○), 10 μM (■), 30 μM (◊), 100 μM (▲) or 150 μM (□) ACh. Insets, the IC_{50} values obtained from individual inhibition curves shown in A and B, were plotted against ACh concentrations for quinine and chloroquine, respectively. The fit of the data to Eq. 4, was done as explained in the text and is shown as a straight line. Note that experimental data for quinine fit to the theoretical curve only at low ACh concentrations, revealing a mixed competitive/noncompetitive behavior. In contrast, chloroquine behaved as a fully competitive antagonist. The mean and S.E.M. of 3 to 6 experiments per point are shown.

Fig. 6. Block by quinine as a function of the membrane potential. A, Representative I-V curves obtained upon application of 2-sec voltage ramps (+50 to -120 mV), 5 sec after the peak response to 300 μM ACh, either alone or in the presence of 10 μM quinine. B, Inhibition of responses to 300 μM ACh in the presence of 10 μM quinine at different holding potentials. Current amplitudes in the presence of quinine plus ACh were obtained from I-V curves as shown in A, and expressed as the percentage of the control current amplitude with 300 μM ACh at each holding potential. The mean and S.E.M. of seven experiments per group are shown.

Molecular Pharmacology Fast Forward. Published on June 13, 2005 as DOI: 10.1124/mol.105.014431
This article has not been copyedited and formatted. The final version may differ from this version.

Fig. 7. Competition radioligand binding to transfected mammalian cells. Cultured mammalian tsA201 cells were cotransfected with subunit chimeras $\alpha9^{(L209)}/5HT_{3A}$ and $\alpha10^{(L206)}/5HT_{3A}$ (in which the extracellular N-terminal domain of the α9 or α10 subunits are fused to the transmembrane and intracellular domain of the mouse $5HT_{3A}$ subunit). Competition binding data with chloroquine, quinine and quinidine is presented as a percentage of [^{3}H]MLA binding obtained in the absence of competing ligand. The curves are from a single experiment but are typical of three independent experiments.

Fig. 8. Effect of chloroquine on ACh-evoked currents in rat cochlear inner hair cells. A, representative traces to ACh either alone or in the presence of chloroquine. B, inhibition curves performed by the co-application of 60 μM ACh and increasing concentrations of chloroquine. Cells were incubated with each concentration of the antagonist for 2 min prior to the addition of ACh. Peak current values are plotted, expressed as the percentage of the peak control current evoked by ACh. The mean and S.E.M. of 5 experiments are shown.

Molecular Pharmacology Fast Forward. Published on June 13, 2005 as DOI: 10.1124/mol.105.014431
This article has not been copyedited and formatted. The final version may differ from this version.

Table 1. Parameters derived from concentration-response curves in the presence of quinine and quinidine.

[μM]	Quinine				Quinidine			
	EC_{50}	max	*H*	n	EC_{50}	max	*H*	n
0	12.4±0.3	0.9±0.1	1.4±0.1	11	14.3±0.5	1.0±0.1	1.1±0.1	12
1	41.8±7.5	1.0±0.1	0.9±0.1	4	24.7±1.5	0.9±0.1	1.4±0.1	5
3	41.3±9.1	0.6±0.1	1.2±0.2	4	25.6±1.8	0.8±0.1	1.5±0.1	4
10	71.4±7.1	0.3±0.1	1.4±0.1	5	32.4±2.4	0.5±0.1	1.7±0.2	6

[μM]: micromolar concentration of either quinine or quinidine; EC_{50}: expressed in μM; max : % of the maximal response to ACh; *H*: Hill coefficient; n= number of experiments.

Molecular Pharmacology Fast Forward. Published on June 13, 2005 as DOI: 10.1124/mol.105.014431
This article has not been copyedited and formatted. The final version may differ from this version.

Table 2. Parameters derived from concentration-response curves in the presence of chloroquine.

[chloroquine] μM	EC_{50}	max	*H*	n
0	13.2±0.3	0.9±0.1	1.2±0.1	11
0.3	30.9±2.1	0.9±0.1	1.4±0.1	4
1	42.2±2.2	1±0.1	1.6±0.1	4
5	171.5±22.9	0.8±0.1	1.2±0.1	4
10	357.2±44.9	0.9±0.1	1.0±0.1	5

EC_{50}: expressed in μM; max : % of the maximal response to ACh; *H*: Hill coefficient; n= number of experiments.

Figure 1

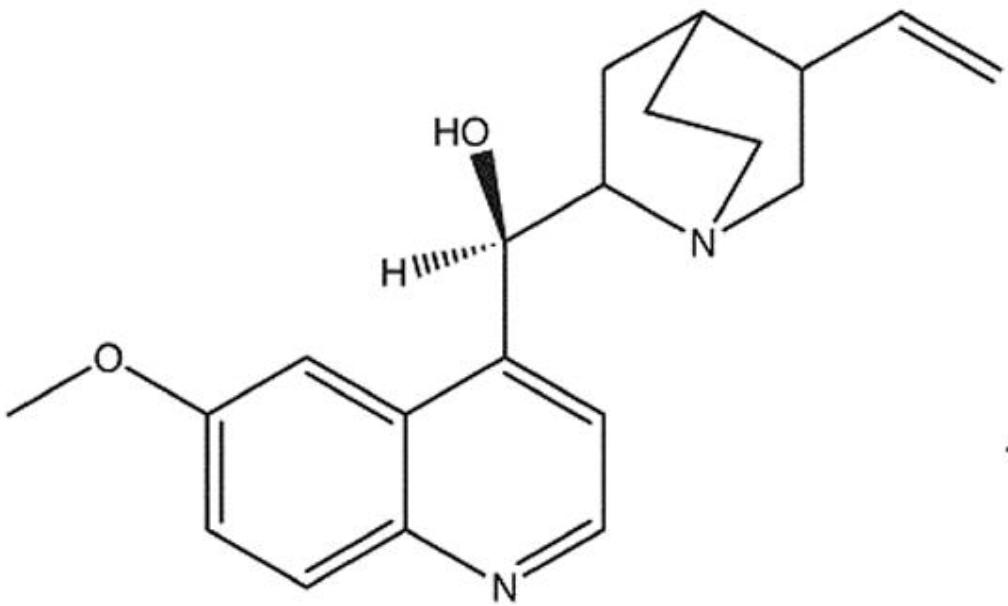

Quinine

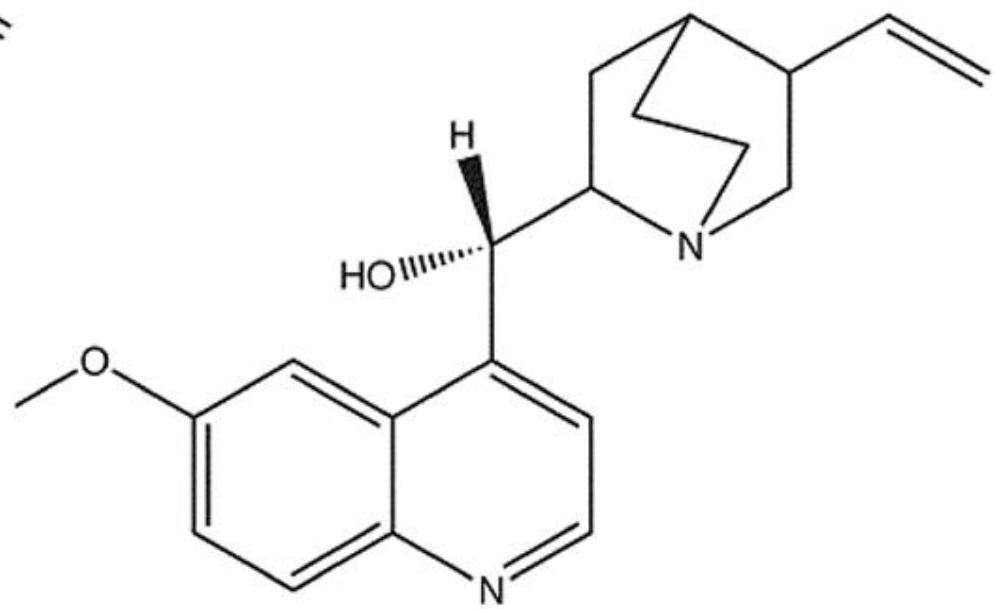

Quinidine

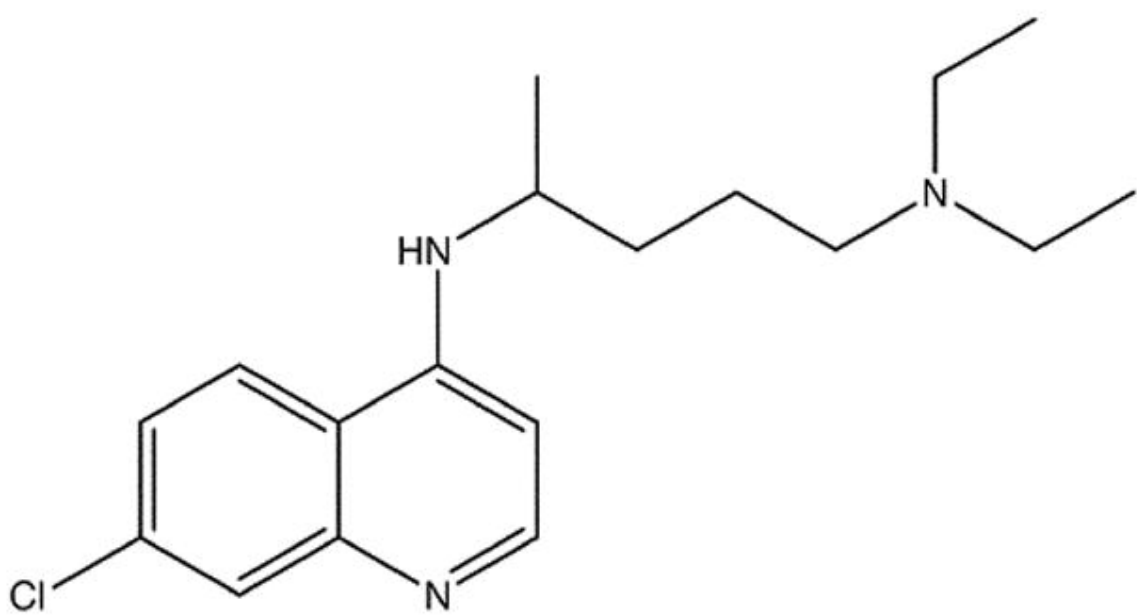

Chloroquine

Figure 2

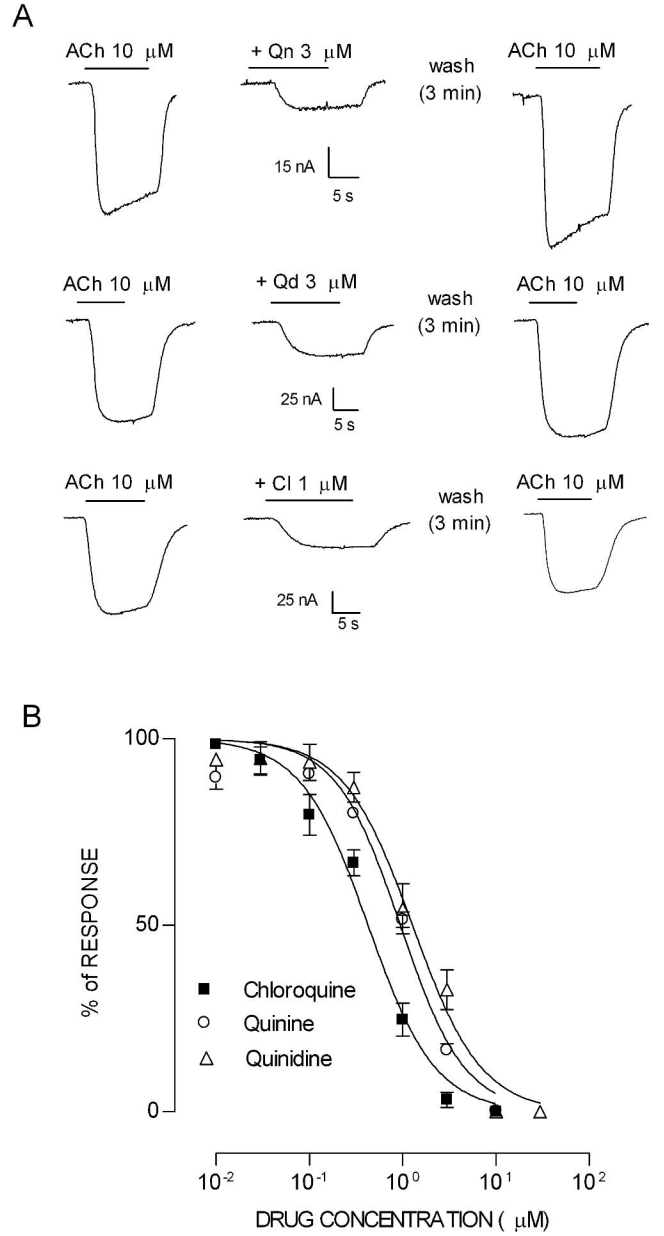
A
ACh 10 μM
+ Qn 3 μM
wash
(3 min)
ACh 10 μM
15 nA
5 s
ACh 10 μM
+ Qd 3 μM
wash
(3 min)
ACh 10 μM
25 nA
5 s
ACh 10 μM
+ Cl 1 μM
wash
(3 min)
ACh 10 μM
25 nA
5 s
B
100
50
0
% of RESPONSE
Chloroquine
Quinine
Quinidine
10-2
10-1
100
101
102
DRUG CONCENTRATION (μM)

Figure 3

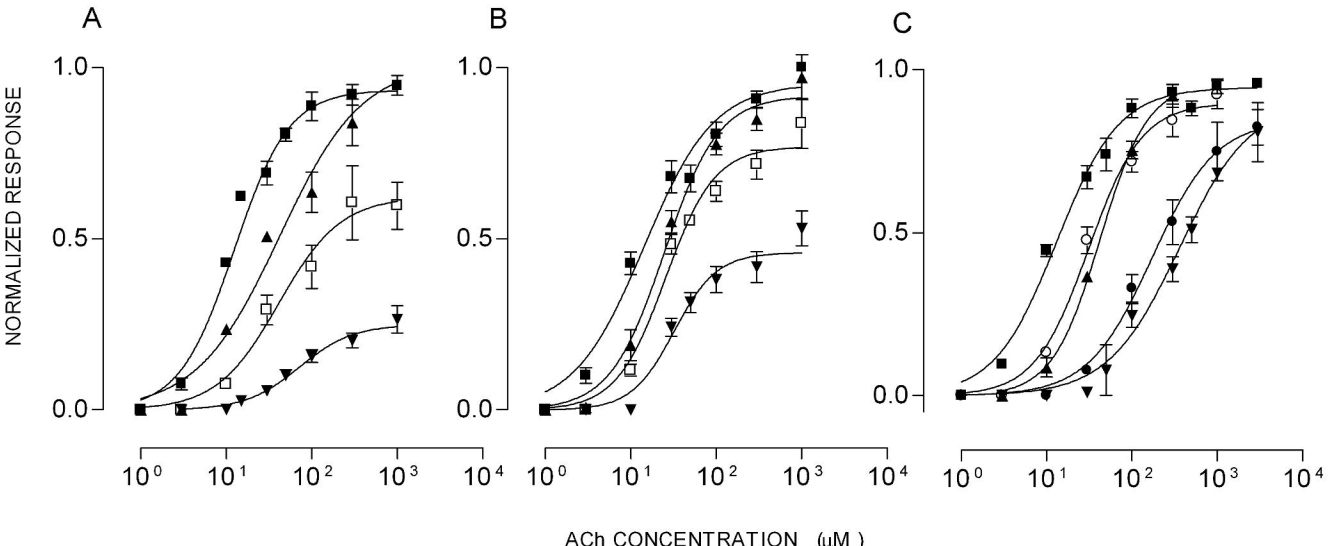
A
B
C
NORMALIZED RESPONSE
1.0
0.5
0.0
10^0
10^1
10^2
10^3
10^4
ACh CONCENTRATION (μM)

Figure 4

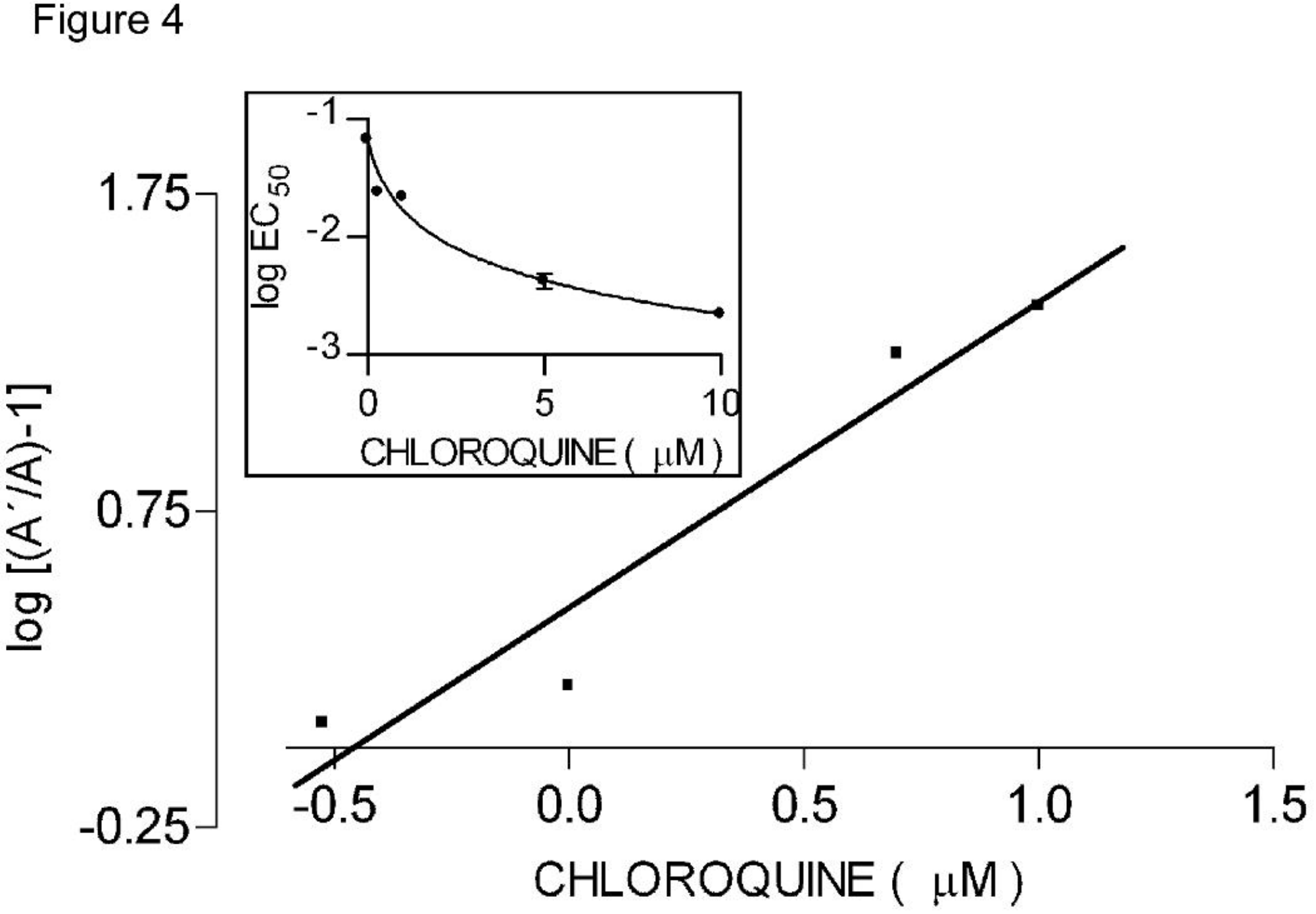
log EC50
-1
-2
-3
0
5
10
CHLOROQUINE (μM)
log [(A´/A)-1]
1.75
0.75
-0.25
-0.5
0.0
0.5
1.0
1.5
CHLOROQUINE (μM)

Figure 5

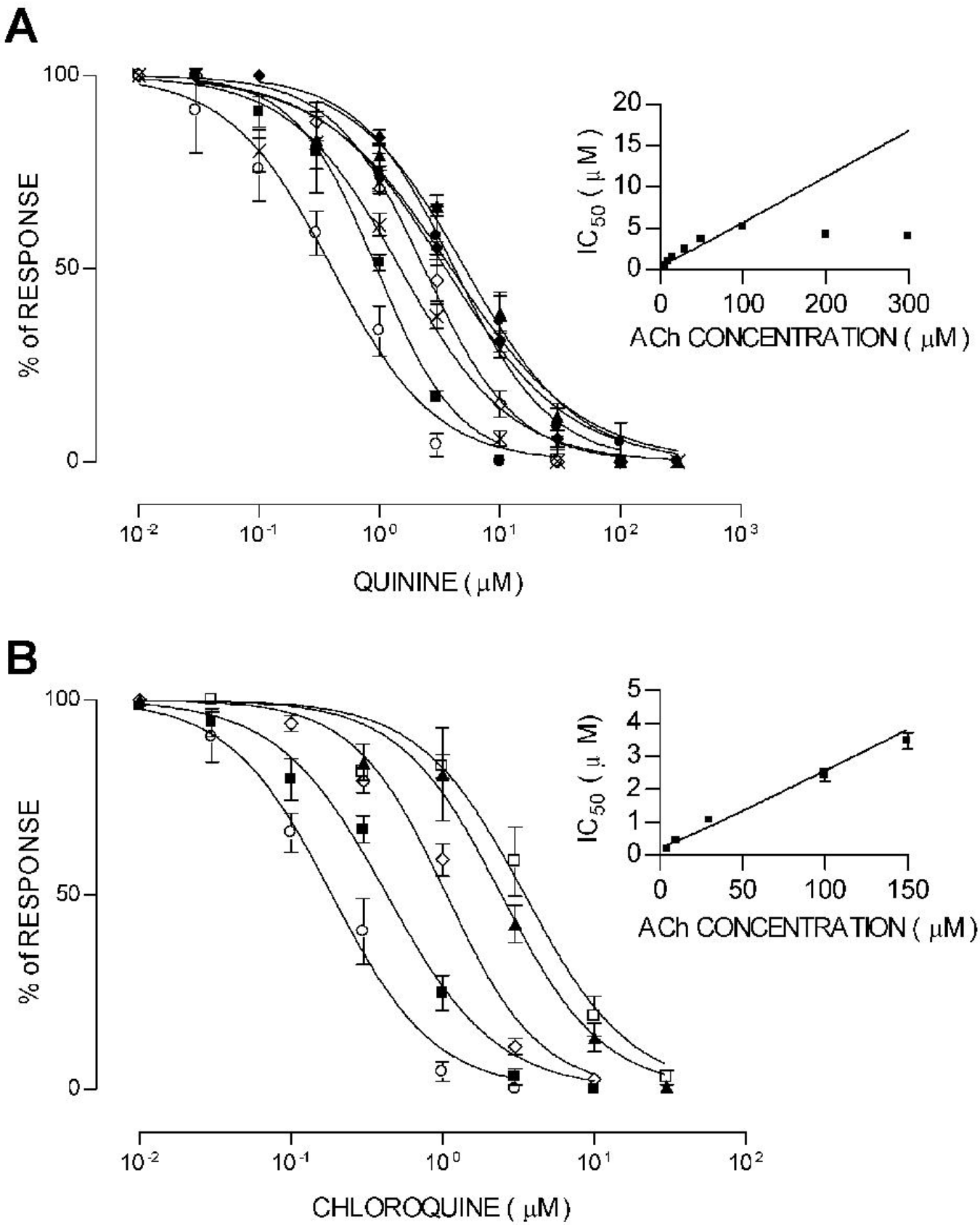
A
100
50
0
% of RESPONSE
10^{-2}
10^{-1}
10^{0}
10^{1}
10^{2}
10^{3}
QUININE (μM)
20
15
10
5
0
IC_{50} (μ M)
0
100
200
300
ACh CONCENTRATION (μM)
B
100
50
0
% of RESPONSE
10^{-2}
10^{-1}
10^{0}
10^{1}
10^{2}
CHLOROQUINE (μM)
5
4
3
2
1
0
IC_{50} (μ M)
0
50
100
150
ACh CONCENTRATION (μM)

Figure 6

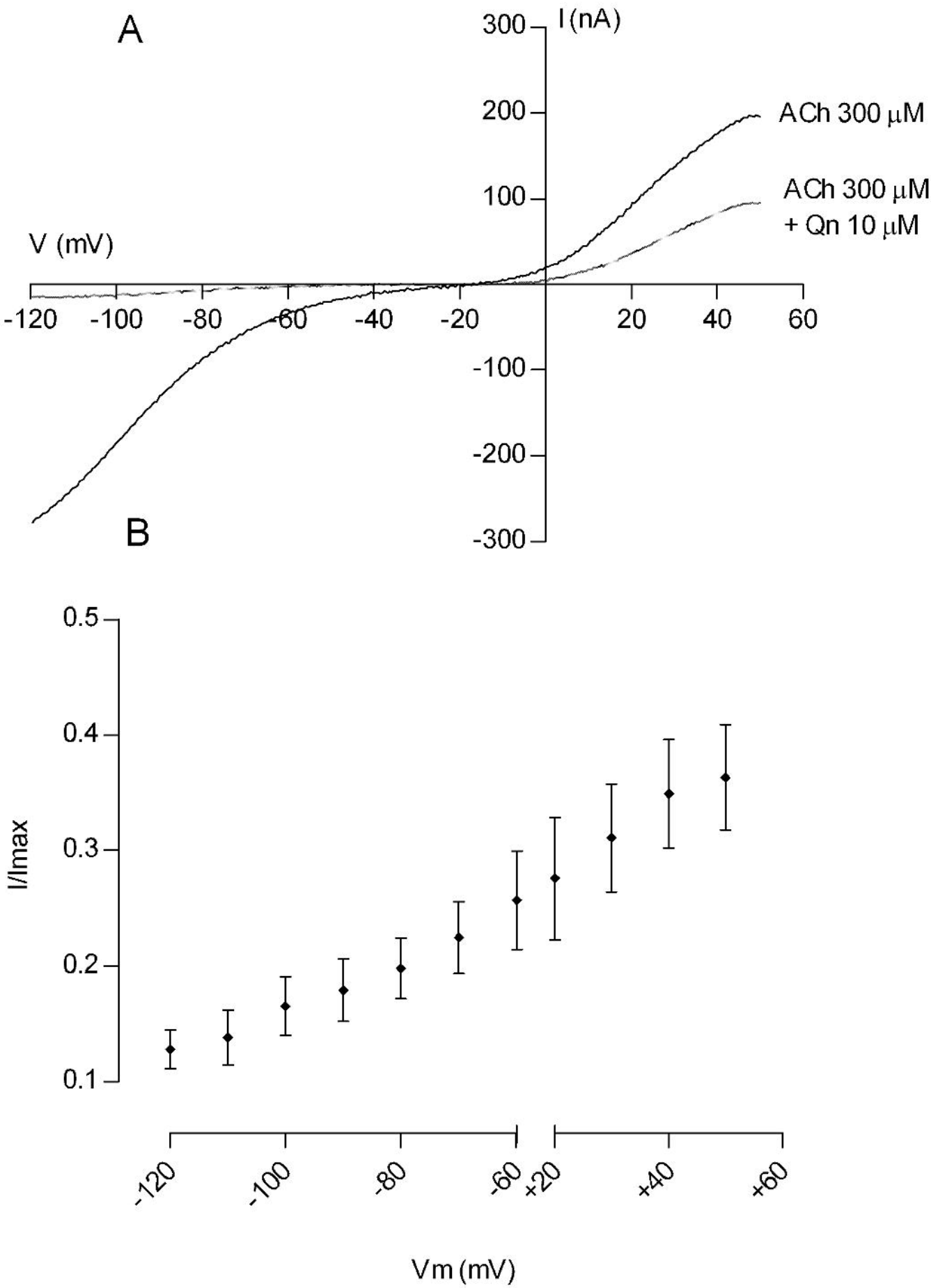
A
I (nA)
300
200
100
-100
-200
-300
ACh 300 μM
ACh 300 μM
+ Qn 10 μM
V (mV)
-120
-100
-80
-60
-40
-20
20
40
60
B
0.5
0.4
0.3
0.2
0.1
I/Imax
-120
-100
-80
-60
+20
+40
+60
Vm (mV)

Figure 7

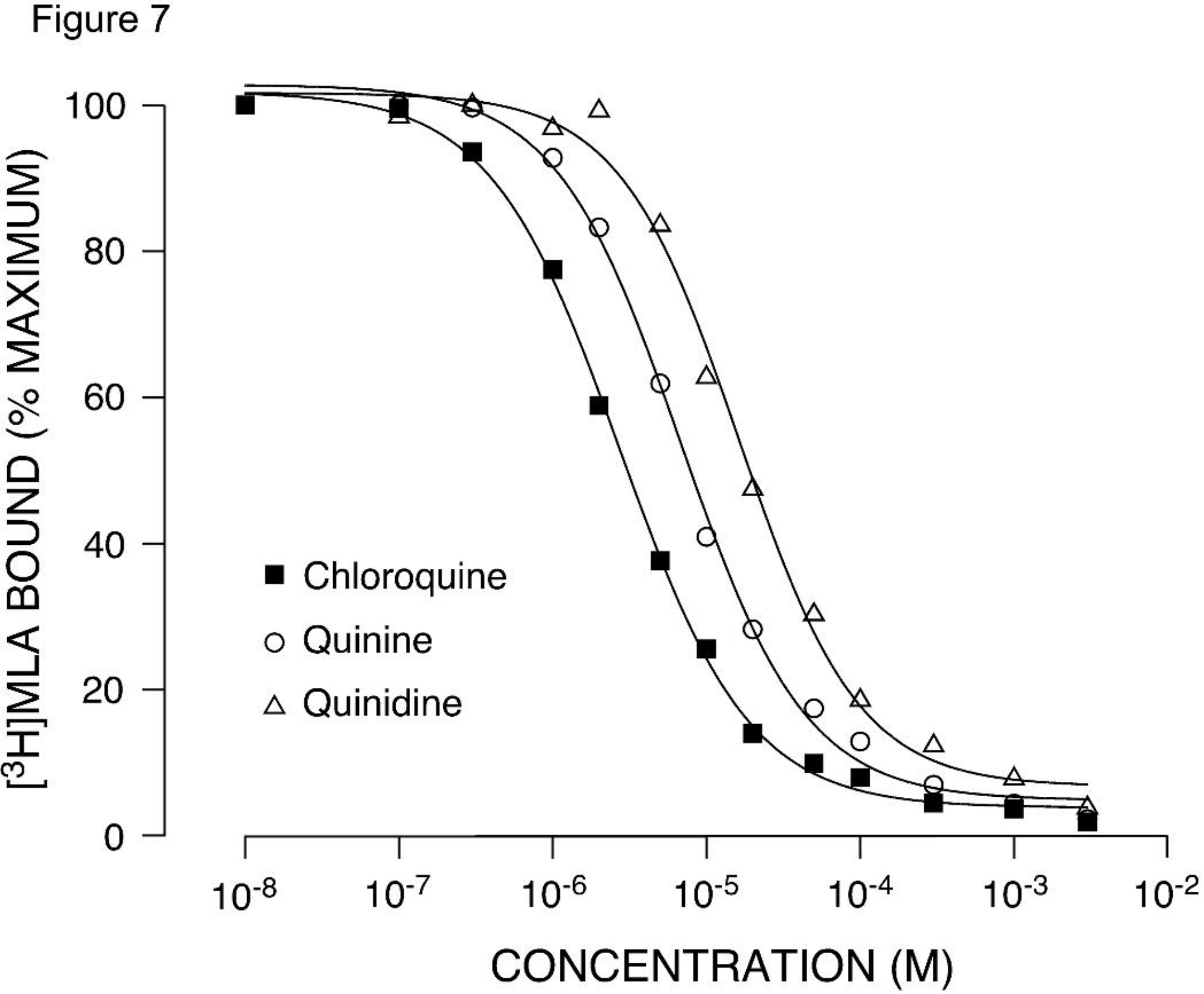
100
80
60
40
20
0
[3H]MLA BOUND (% MAXIMUM)
Chloroquine
Quinine
Quinidine
10-8
10-7
10-6
10-5
10-4
10-3
10-2
CONCENTRATION (M)

Figure 8

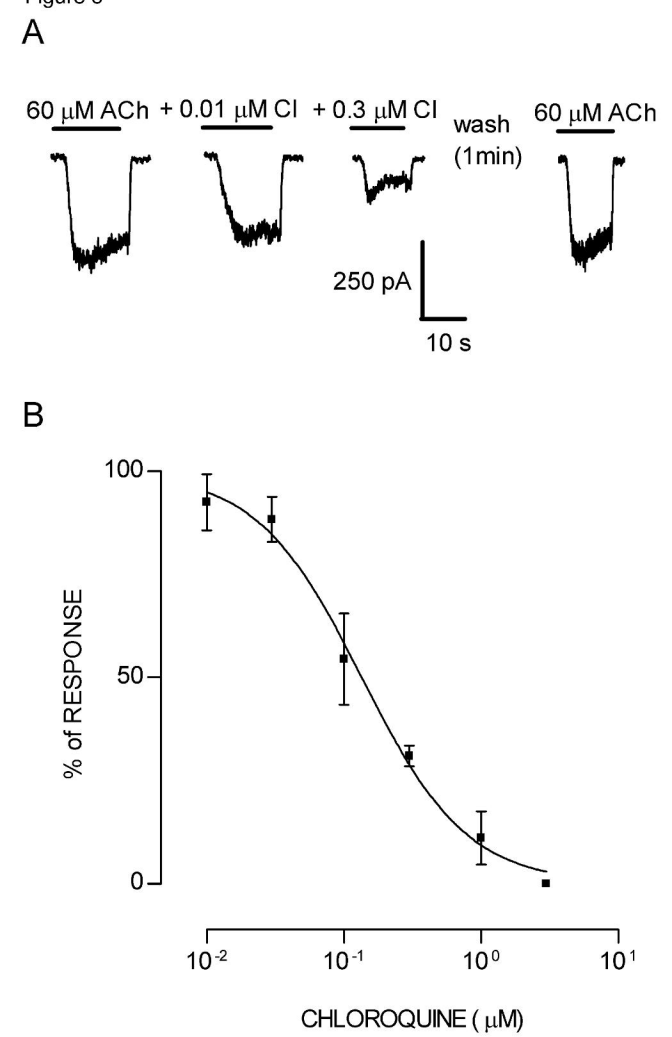
A
60 μM ACh
+ 0.01 μM Cl
+ 0.3 μM Cl
wash
(1min)
60 μM ACh
250 pA
10 s
B
100
50
0
% of RESPONSE
10-2
10-1
100
101
CHLOROQUINE (μM)